Heliodyne Corporation

Research Note 15 June 1964

Progress on SAPAG Facility, III

Roy S. Hickman, Horace A. Ory
and I. R. Tannenbaum

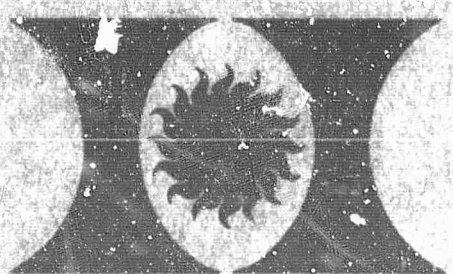

RESEARCH NOTE 15

PROGRESS ON SAPAG FACILITY, III

by Roy S. Hickman, Horace A. Ory, and I. R. Tannenbaum

HELIODYNE CORPORATION
Los Angeles, California 90064

June, 1964

prepared for

ADVANCED RESEARCH PROJECTS AGENCY

under ARPA Order 360-62
monitored by the
U.S. ARMY ORDNANCE MISSILE COMMAND
Redstone Arsenal, Alabama

under Contract No. DA-04-495-ORD-3574(Z)

This research is a part of Project DEFENDER, sponsored by the Advanced Research Projects Agency, Department of Defense

BLANK PAGE

Progress on SAPAG Facility, III*

by
Roy S. Hickman, Horace A. Ory, and I. R. Tannenbaum
Heliodyne Corporation
Los Angeles, California 90064

ABSTRACT

This Research Note covers progress in the SAPAG experiment during the reporting period. Refinements in apparatus and techniques for the production of ultra-fine particles, particularly of organic ablators, are described. Representative photomicrographs of powder preparations, as well as number density distribution curves, are presented and discussed. The results of light scattering investigations of aerosol distribution and stability are analyzed. Further modifications to the facility, based in part on the results of the above studies, and further development of instrumentation, are also included.

*This research is a part of Project DEFENDER, sponsored by the Advanced Research Projects Agency, Department of Defense, under ARPA Order No. 360-62.

TABLE OF CONTENTS

1. INTRODUCTION

Heliodyne Corporation is investigating the ionization and radiation properties of reentry vehicle materials under conditions which simulate those of actual flight. The experimental program involves the preparation of representative materials into sub-micron sized particles under carefully controlled conditions, the injection of these particles into a shock tube, and the measurement of electron density and radiation as a function of distance behind the shock. From the results obtained, the chemical kinetics of the ablation process and the phenomenology of reentry observables can be elucidated.

The pulverized material must be injected as sub-micron particles so that good dispersion is obtained and the difficult fluid mechanics can be decoupled from the shock induced ablation reactions. The development of methods for preparation of ultra-fine particles is essentially complete, and is described in Section 2, where electron photomicrographs and number density distribution curves of comminuted material are presented and discussed.

Light scattering investigations of the efficiency of methods developed for particle injection, and of the uniformity and stability of the aerosol produced, are reported in Section 3. The results confirm the validity of current injection techniques, and show that horizontal shock tube operation is practicable under certain conditions.

In Section 4, recent modifications to the shock tube are described; these include adaptations for horizontal operation, the insertion of a vapor barrier to eliminate contaminants from portions of the injector, and various changes that have led to much improved

vacuum operation.

Considerable extension of shock tube instrumentation, described in Section 5, has made possible more efficient and comprehensive data acquisition.

RN15, 6-64

2. COMMINUTION

The preparation of the ultrafine powders required for use in the SAPAG facility has been carried out successfully both at room temperature and at cryogenic temperatures. Comminution at room temperature has been successful for those materials which are sufficiently brittle, while the more rubbery substances have been found to comminute only at relatively low temperatures.

2.1 Experimental

2.1.1 Apparatus

Two instruments have been designed and constructed in order to produce the required powder. The cryogenic ball mill can be used both at high and low temperatures and is capable of producing approximately 20 grams of submicron sized powder per day. It is constructed of stainless steel and uses stainless steel balls as impactors. The grinding chamber is machined smooth and has no sharp corners so that cleaning is easily accomplished to minimize the level of contamination between loadings. The grinding chamber is hermetically sealed so that the powder is always maintained in a controlled atmosphere.

The other device being used for the production at ultra-fine powder is the high energy harmonic impactor. This machine, currently in prototype form, is capable of producing only approximately four grams of comminuted material per day due to its small size. It is, however, being scaled up by more than a factor of ten so that the output of this machine is expected to rise to more than 40 grams daily.

The grinding in the impactor is very rapid. All materials studied to date have been reduced to micron-sized particles in less

than 20 minutes. The principle upon which this impactor operates is the acceleration of attritors within a crucible so that the kinetic energy of the attritors is transferred to the particles being comminuted, thereby breaking them up. The attritors can either be steel balls or can be large pieces of the material being ground. When the material being ground has sufficient structural strength, the crucible can be made of the same material so that contamination by the crucible and the attritors can be reduced to zero from the very low value observed when steel is used in these applications.

Since materials with particles in the micron and sub-micron size range have a very large surface area, they are very easily contaminated by absorption of gases from the atmosphere which they contact. Accordingly, all materials other than in bulk form are handled only in a controlled, inert atmosphere dry box, a photograph of which is shown in Figure 1. Thus, the observed properties of the particulate matter will be due only to the interaction of the shocked gases with the material without any effect due to absorbed gases.

2.1.2 Materials

Real ablation materials are currently being ground to micron particle size in the equipment described in the

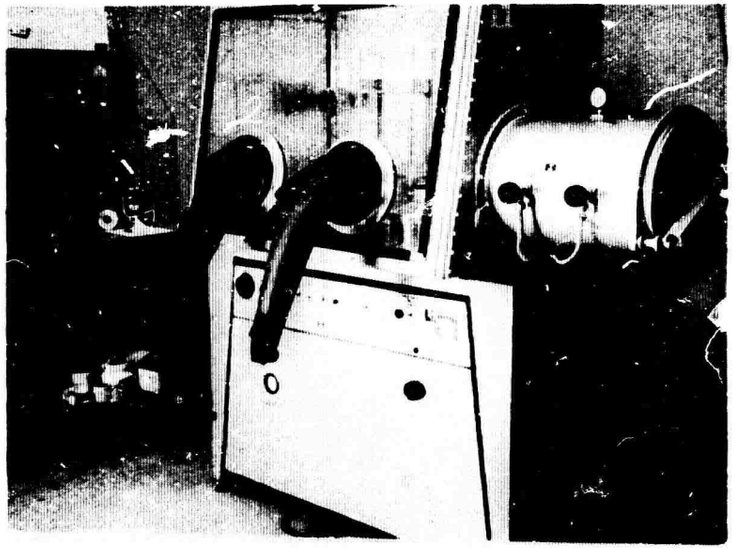

Fig. 1 Inert atmosphere dry box which is used to minimize contamination of fine powders. The gas used in the dry box is nitrogen from which the oxygen is removed by catalytic reaction with hydrogen, and water vapor is removed by adsorption on a molecular sieve. The typical level of contamination in this dry box is less than 3 ppm water as read on an electrolytic moisture detector. The oxygen level is sufficiently low that a tungsten filament bulb can be maintained incandescent for days unprotected without failure.

preceding section. These operational ablation materials exhibit widely varying physical properties. Some are brittle at room temperatures so that they may be pulverized easily without the necessity of using low temperatures. Others, however, are rubbery in nature so that pulverization can occur only at low temperatures. Futhermore, other materials are composites, so that the possibility of obtaining two separate size distributions is present.

2.2 Results and Discussion

The marked effect of moisture upon the finely divided materials is shown in Figure 2. This figure shows the powder obtained from the high energy harmonic impactor both when the comminution of Avcoat II is carried out in room air and when performed completely in an inert atmosphere. It is clear that processing of materials in a moist atmosphere yields a product which agglomerates very markedly; a finely divided powder is obtained by removing the moisture from the atmosphere.

Figure 3 shows optical photomicrographs of the powder shown macroscopically in Figure 2. It can easily be seen that the dry grinding gives a much smaller average particle size than the same procedure produces when moisture is present.

Figure 4 shows an optical photomicrograph of a fiber glass filled phenolic graphite after being treated for one minute in the high energy harmonic impactor. The presence of the fiberglass phase is very clearly shown.

Figure 5 is an optical photomicrograph of the same material as shown in Figure 4 after an additional 19 minutes in the impactor. The absence of the large particles of the glass phase is illustrated

Fig. 2 Results of comminution of Avcoat II in the high energy harmonic impactor. The photograph on the left shows the material after being ground in room air. Note that the steel ball used for the comminution is covered by an adherent mass of ground material.

The photograph on the right shows the results of the comminution of the same material in the same equipment, the only change from the above being the replacement of moist air with an inert dry atmosphere. In this case the powder shows no tendency to stick to the ball or to form large agglomerates.

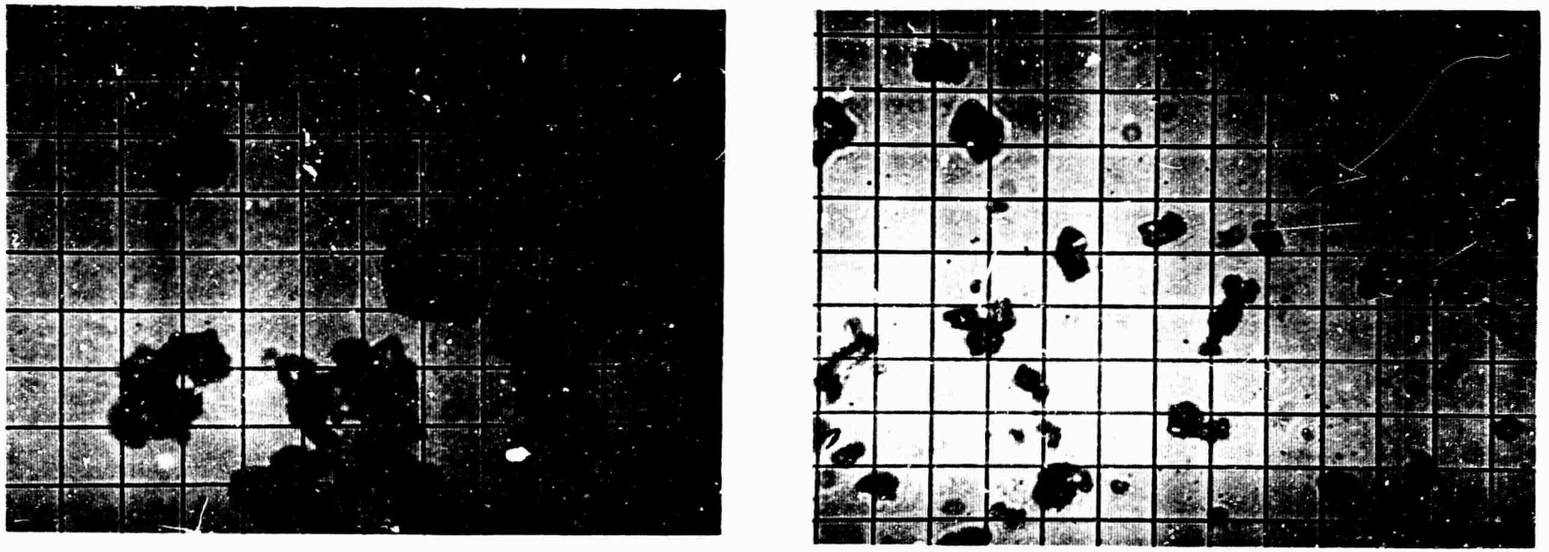

Fig. 3 Optical photomicrographs of Avcoat II after comminution in the high energy impactor. Each square represents 5 microns. The photomicrograph on the left, of moist material, shows the presence of large agglomerates. The photomicrograph on the right, of dry material, shows the presence of relatively small particles and the complete absence of the very large agglomerates o. the moist material.

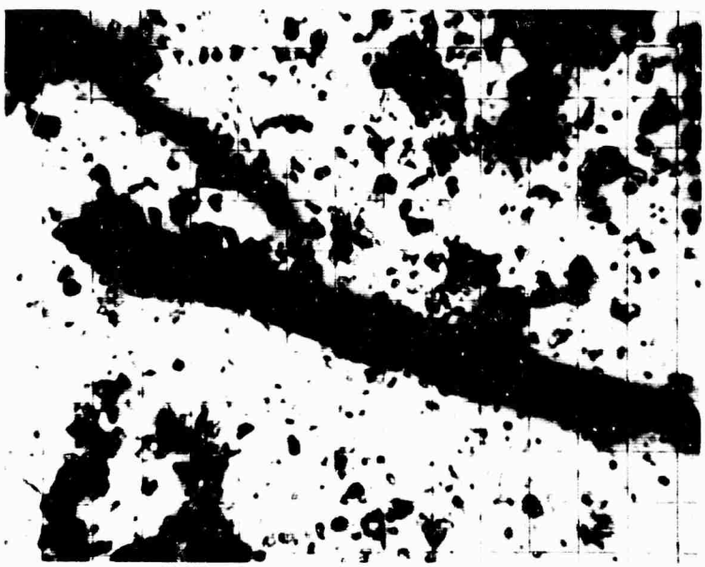

Fig. 4 Optical photomicrograph of a phenolic graphite treated for one minute in the high energy harmonic impactor in a dry atmosphere. Each square represents 5 microns. The presence of the fiber-glass phase is easily seen as the rod that runs diagonally across the photomicrograph.

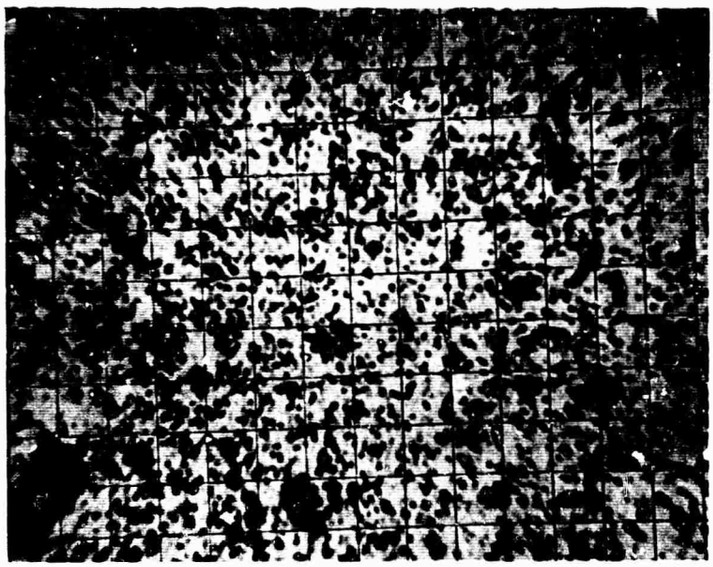

Fig. 5 Optical photomicrograph of phenolic graphite after 20 minutes in the high energy harmonic impactor in a dry atmosphere. Each square represents 11 microns. Both phases have been comminuted to the limit of detection by optical microscopy.

as well.

Figure 6 is an electron micrograph of the same material shown in Figure 5. The presence of the two phases is apparent in this picture as is the very small size of the particles.

A statistical analysis of this sample has been made by completely counting the particles from twelve randomly sampled electron micrographs. The results are shown in Table I and are plotted in Figures 7 and 8. Two phases are easily discernible, the large non-transparent material and the smaller, transparent phase, arising from the glass and phenolic phases, respectively.

Among the other materials undergoing comminution for use in the SAPAG experiment is an epoxy resin. Electron micrographs of this material treated for seventy two hours at room temperature in the cryogenic ball mill are presented in Figures 8 and 9. The presence of particulate matter with major dimension of 0.2 microns is shown to be present. The electron micrographs also show the loose agglomeration of small particles to form larger groupings. The average particle size for the material shown in Figures 9 and 10 is approximately 0.5 microns, well within the requirements of SAPAG.

The possibility of contamination by comminution in a steel apparatus has also been studied by spectroscopic determination of the presence of the metallic elements both before and after treatment. Although the level of contamination of the metallic elements appears to increase, the increase is comparable to the very small amount present initially (typically, e.g., for iron from 1.9 ppm to 3.1 ppm after 72 hours in the ball mill) so that the reliability of these measurements have not yet been fully assessed. In any case, the absolute amount of contaminant is very small.

TABLE I

PARTICLE SIZE ANALYSIS FOR PHENOLIC GRAPHITE

PARTICLE SIZE	SMALL PARTICLES		LARGE PARTICLES		TOTAL PARTICLES	
	Increment of Count (%)	% Greater Than	Increment of Count (%)	% Greater Than	Increment of Count (%)	% Greater Than
μ						
0.08-0.1	24.02	75.98	14.52	98.54	21.44	78.56
0.1-0.2	20.42	55.56	22.58	62.90	21.01	57.55
0.2-0.3	20.42	35.14	13.71	49.19	18.60	38.95
0. .4	13.81	21.33	6.45	42.74	11.82	27.13
0.4-0.5	7.51	13.82	7.26	35.48	7.44	19.69
0.5-0.6	9.31	4.51	9.68	25.80	9.41	10.28
0.6-0.7	2.40	2.11	8.06	17.74	3.94	6.34
0.7-0.8	1.20	0.91	8.11	16.93	1.09	5.25
0.8-0.9	0.30	0.61	6.45	10.48	1.97	3.28
0.9-1.0	0.60	0	2.42	8.06	1.09	2.19
1 - 2			4.84	3.22	1.31	0.88
2 - 3			2.42	0.80	0.66	0.22
3 - 4			0.81	0	0.22	0

Fig. 6 Electron micrograph of glass-filled phenolic graphite at a magnification of 22000X. The very small particle size is shown, as is the presence of two phases. The statistical particle size analysis based upon this photograph and eleven others is presented in Fig. 7 and 8.

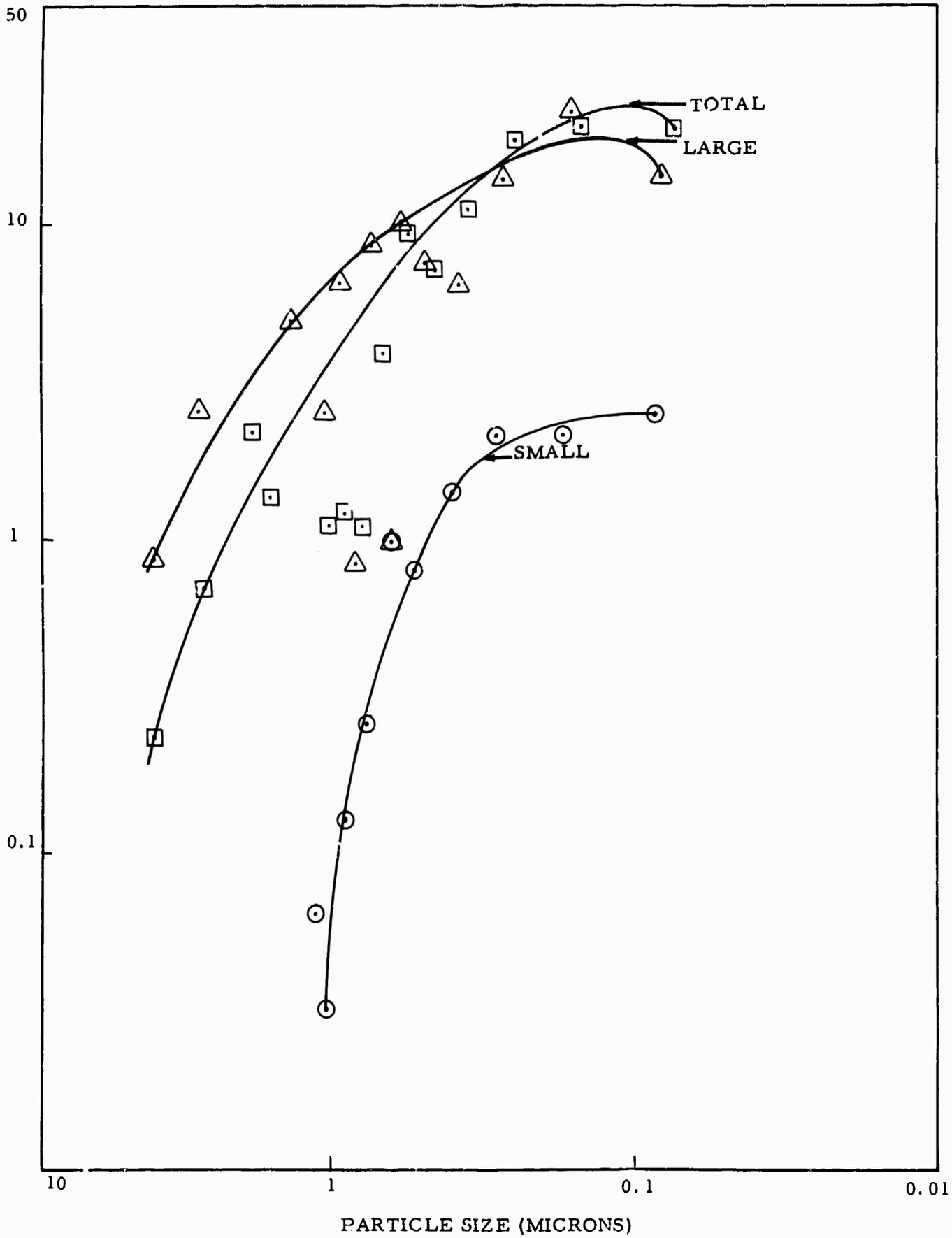

Fig. 7 Particle size analysis for phenolic graphite. This differential distribution curve for material shown in Figure 6 is obtained by counting all the particles on 12 electron micrographs. Note the presence of large amounts of particles in the submicron range.

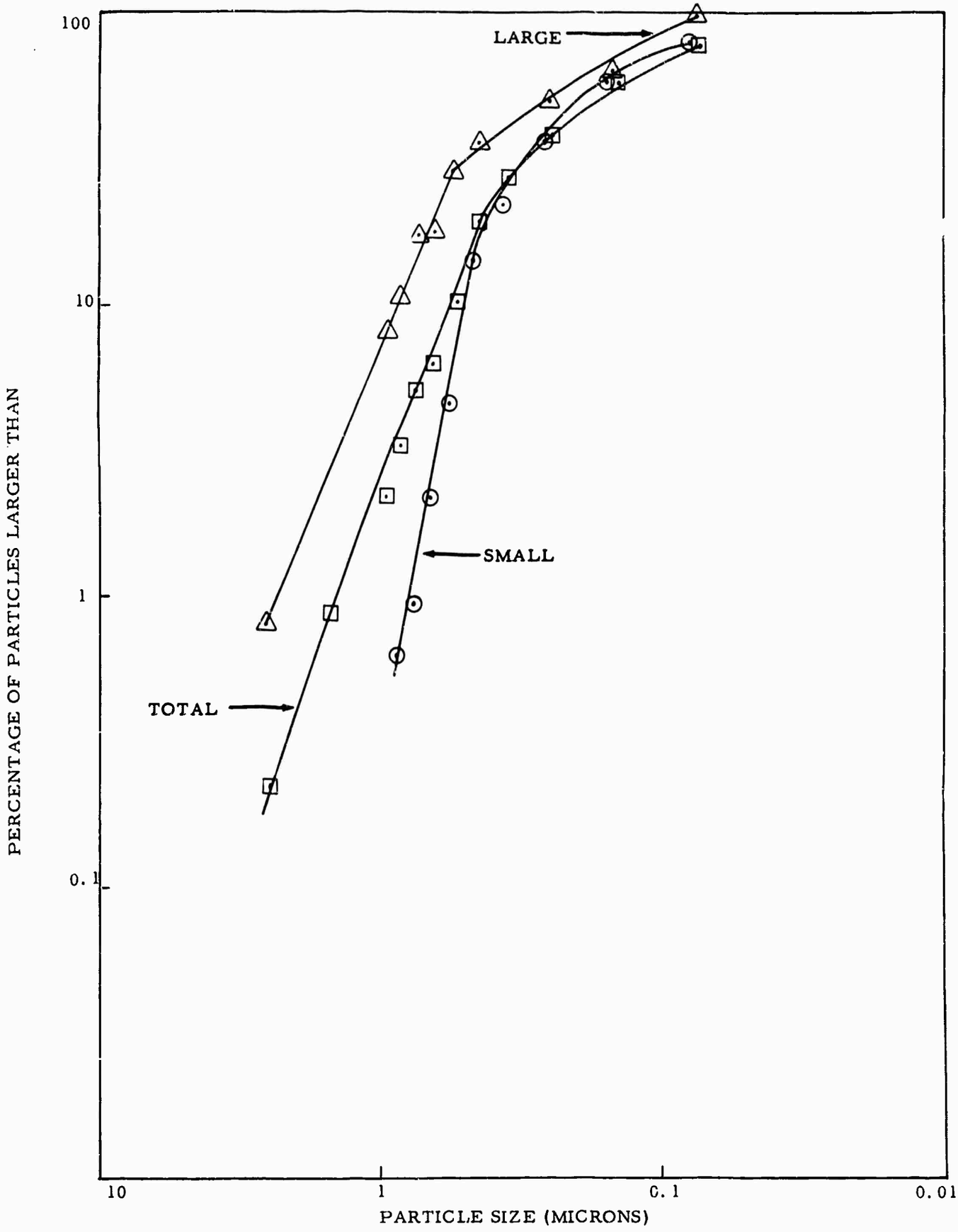

Fig. 8 Particle size analysis for phenolic graphite. This intergral distribution curve for material shown in Figure 6 is obtained from the data plotted in Figure 7.

Fig. 9 Electron micrograph of an epoxy resin comminuted 72 hours at room temperature in the cryogenic ball mill (magnification is 15000X). The presence of small particles (0.2 microns) is shown. Similarly, the loose agglomeration of the small particles can be seen in this micrograph.

Fig. 10 Electron micrograph of an epoxy resin comminuted 72 hours at room temperature in the cryogenic ball mill (magnification is 15000X). The presence of small particles (0.2 microns) is shown. Similarly, the loose agglomeration of the small particles can be seen in this micrograph.

BLANK PAGE

3. POWDER INJECTION

In order to make the SAPAG device easier to handle, and in order to use standard shock tube techniques, it is highly desirable to place the shock tube in a horizontal position. This horizontal arrangement compounds the problem of dust injection because the powder injected into the tube is expected to gravitate to the bottom of the tube soon after injection. In fact, there are some questions as to whether or not a uniform dust mixture can ever be obtained in such a facility. In order to check these features and to gain experience in a horizonal dust injection device, a glass tube was set up in one of the laboratories with an injector arranged at one end. A light source was built which projected a narrow beam of light down the axis of the tube. The dust concentration was monitored as a function of time and position by using photomultipliers and oscilloscopes.

3.1 Experimental Procedure

3.1.1 Scattering Apparatus

An enclosed 300 watt carbon arc was used to illuminate a .030 diameter pin hole which in turn illuminated a collimating lens. The lens, pin hole and light source were arranged so that a half inch diameter collimated beam of light was produced. This beam of light was chopped at 42 cycles per second so that the signal picked up by the photo detector could be amplified by an ac amplifier (see Fig. 11). The entire light system was placed on the horizontal plane below the shock tube. The light beam was reflected vertically to a second mirror which directed the light down the axis of the tube. This arrangement was used so

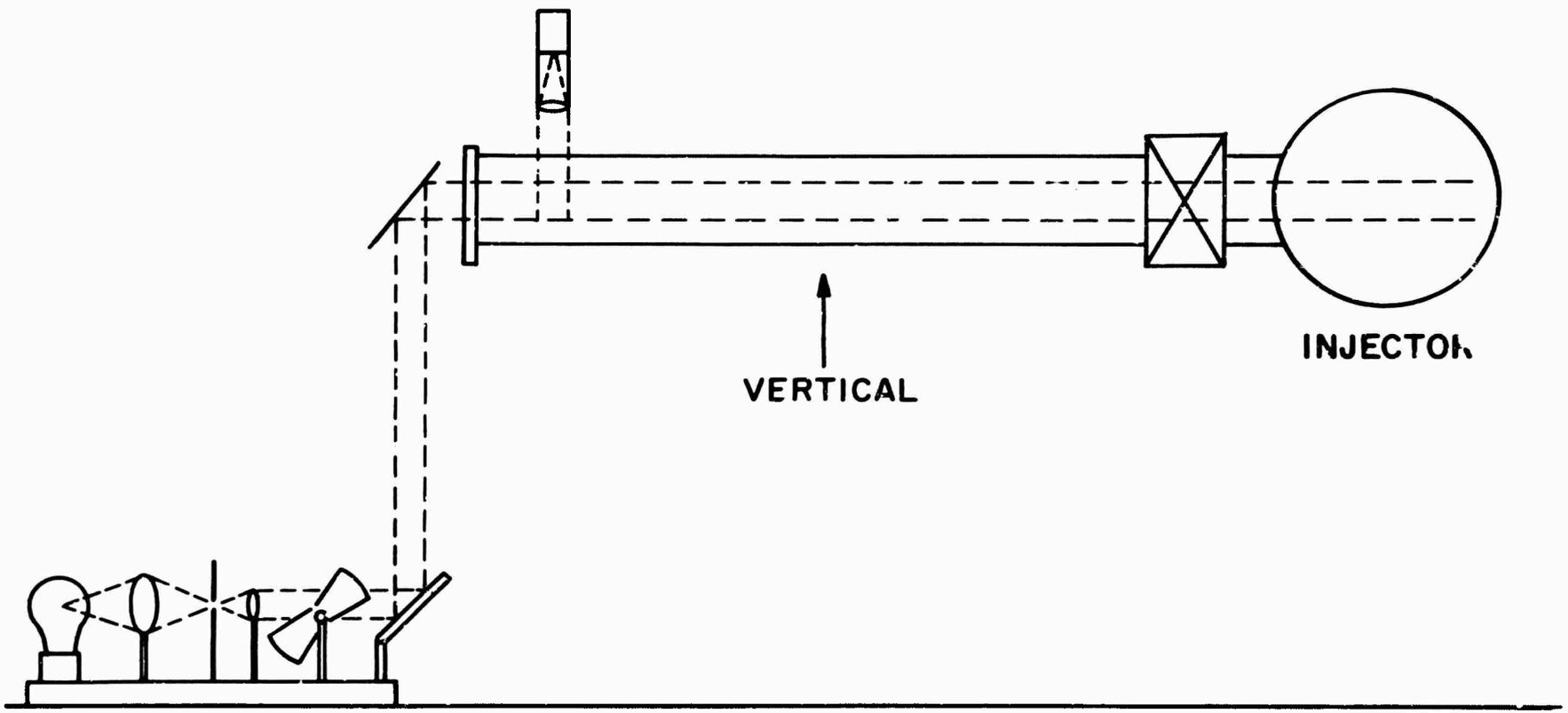

Fig. 11 Schematic of the light scattering experimental arrangement. A 300 watt enclosed carbon arc was used to illuminate the tube. The dusty gas was passed through the valve between the injector and the tube. The scattered light could be monitored at any point along the tube.

that an axial movement of the light source produced a vertical scan in the tube itself. A photomultiplier tube was located at different positions along the axis of the galss tube. For all the tests the photomultiplier was run at 900 volts. It is found that some flicker existed in the light source; however, over a period of one to two seconds very little change was observed in its integrated behavior. In order to monitor the total amount of light which was beamed from the light source, the photo tube used in the test was located directly above the first mirror in the vertical portion of the light path. Two neutral density filters were placed in front of the photo-tube which reduced the light intensity by a factor of 1×10^5. In this manner the electronics were kept the same so that absolute calibrations on the phototube were unnecessary. For every experimental shot the initial energy coming from the first mirror was measured. No corrections were made for the light lost in the second mirror or in the lucite entrance window, however, it is felt that the amount of light which was lost is not considerable.

3.1.2 Experimental Data

The experiment was performed as follows: first the entire tube and injector were thoroughly cleaned with acetone, then 7 grams of teflon TFE 120, was placed in the injector sieve. Then the entire unit was sealed and was pumped down to less than 10 microns. Sufficient time was allowed for the dust to outgas and for any acetone present in the system to outgas and be pumped away. The main valve was closed so that the tube was isolated from the in jector and the pressure in the injector was raised to 1.25 cm Hg. Then the light source was turned on, the lights in the room were turned off and the

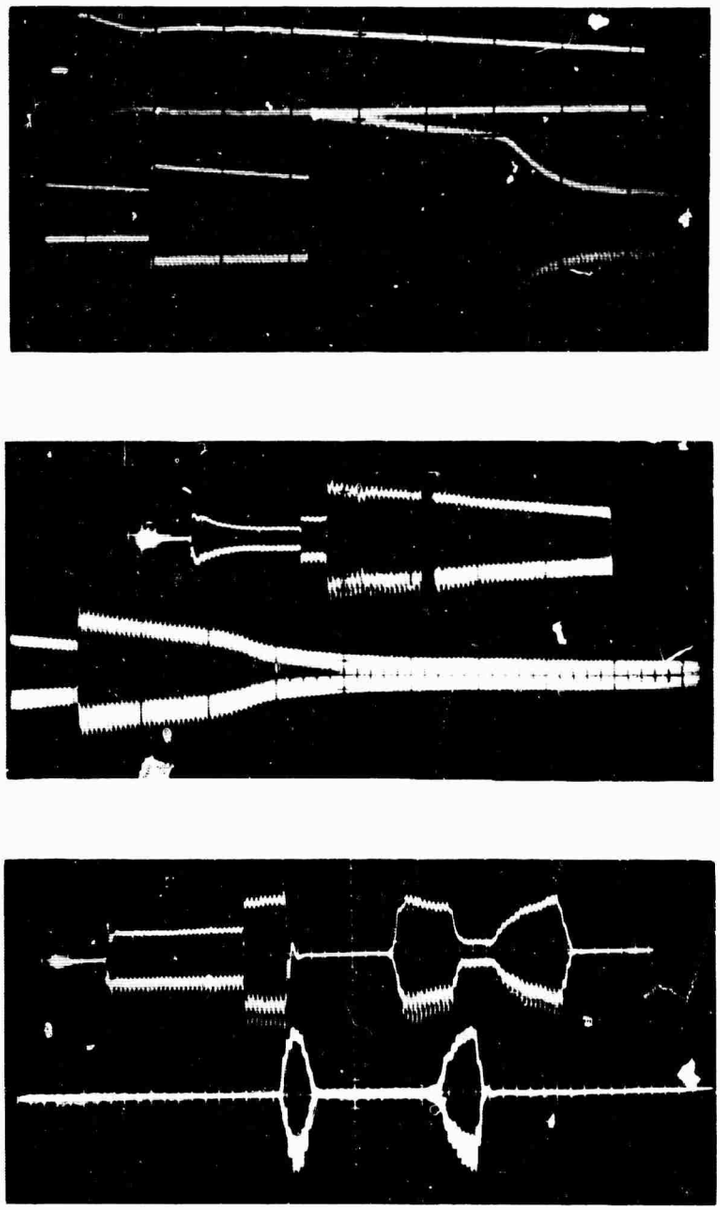

Fig. 12 Records of data taken with the arrangement of Fig. 11, with the light beam at the (a) center, (b) top, and (c) bottom of the tube. The sharp increases in the traces are caused by changes in the attenuation on the amplifier. In (c) the light beam scanned the tube after 25 seconds, with a scope sweep rate of 5 seconds per centimeter. Note the relatively constant scattering signal at early times. In (a) the early scattering signal decreases slowly, and in (b) it decreases rapidly. This is caused by particles leaving the field of view from the top of the tube; particles lost from the bottom are made up by particles falling from higher positions.

photomultiplier was turned on. The fan was started in the injector and the speaker was oscillated at 30 cycles per second. After all the dust had been shaken from the sieve and was thoroughly stirred in the injector, the main valve was opened and the tube filled with dust. Just prior to opening the main valve the sweep was started on the oscilloscope. Thus, the short time decay of number density was monitored.

Figure 12 shows three sets of data. Figure 12A is a trace taken with the photomultiplier located 12 inches from the end plate. The light beam is located exactly on the center of the trace. The first burst of light is seen when the injector valve is opened. Then a very short term decay of scattering is seen followed by a relatively long period (ten to fifteen seconds) of very uniform scattering. After about fifteen seconds one can see that the trace is no longer flat and begins to decay in almost a linear fashion. This is attributed to the end of the passage of the largest particle sizes contained in the sample which started at the top of the tube. Once the dust is injected into the tube all of the particles begin to fall immediately. If ripples occur in the trace non-uniformities in the vertical directions are indicated.

The lower set of traces in each photo was triggered after a fifty second delay. The first radical jump in the trace is where an attenuator switch was changed from a times ten attenuation to a times five attenuation. The scope gain was 1/2v/cm. The second jump is where the attenuation was changed from times five to times two. Near the end of the bottom set of traces one can see a sharp decline in the scattered light. This is caused by the opening of a pump-out valve which extracts all of the gas remaining in the tube. This was done to obtain the mass loading in the tube.

Figure 12B is a trace obtained in exactly the same fashion with the light beam located one inch above the center line of the tube. In this case the gain in the scope is one volt per centimeter starting with a times ten attenuation, then changing to a times five, then a times two, and then times one.

Figure 12C is a trace obtained one inch below the center line of the tube. It starts out with a one volt per centimeter and shifts from times ten to a times five attenuatuation and immediately thereafter the light beam is manually turned off. This is done by blocking the light beam. The first burst of signal following this is when the light beam is made to traverse from the bottom of the tube to the top. As can be seen a decrement of about ten to fifteen percent occurs in this traverse. Immediately thereafter, the light source was dragged back and the signal can be seen to again change by about twenty percent. The gradual increase from zero signal to the plateau signal is caused by misalignment of the light and scattering from the side wall, so that it is dependent on the time which the operator takes to scan the tube. Much later in the second set of traces a similar scan was made very rapidly and finally a similar scan was made from the top to the bottom. As can be seen, as time goes on, the level of the light scattered by the gas near the bottom of the tube does not change much from the initial values; however, the light scattering from the top of the tube is seen to decrease fairly rapidly. This is exactly what one would expect in a settling dust cloud containing many different size particles, because the large particles fall through the tube and the particules in the bottom of the tube which were initially there continue to fall out but are replenished by dust falling from

the upper portions of the tube. The space near the top of the tube loses its large particles and has no supply above it, thus the upper portions of the tube show a decrease in scattered light whereas the bottom portions do not. The fact that the scattered light from the bottom sections of the tube changes little indicates that the number density distribution is uniform in height across the tube, that is, the number of large particles falling into the lower volume of the tube equals the number of particles falling out of the lower volume of the tube. If the portions of the tube near the top contained either more or fewer particles of a given size, the scattered light from the bottom portion of the tube would be seen to change more rapidly.

In addition to the detailed investigation of the vertical distribution in the tube, a set of measurements was made along the center line of the tube down the axis of the tube. The results of these measurements are shown in Figure 13 where the apparent brightness of the dust cloud is plotted as a function of position along the tube. This curve is a plot of the light being scattered by the dust in the tube. If the turbidity or the number density per unit volume times a particle area times a scattering coefficient is constant this line should be an exponential decrease. If there are number density variations along the tube then the slope of the experimental curve should deviate as one moves along the beam path, because the decrease in light scattered should vary as the number density or as the turbidity. The fact that this does not occur and there is a relatively smooth decrease of brightness indicates that the dust is uniform along the tube. Each section of the tube is behaving just as each section in front of it. This indicates that

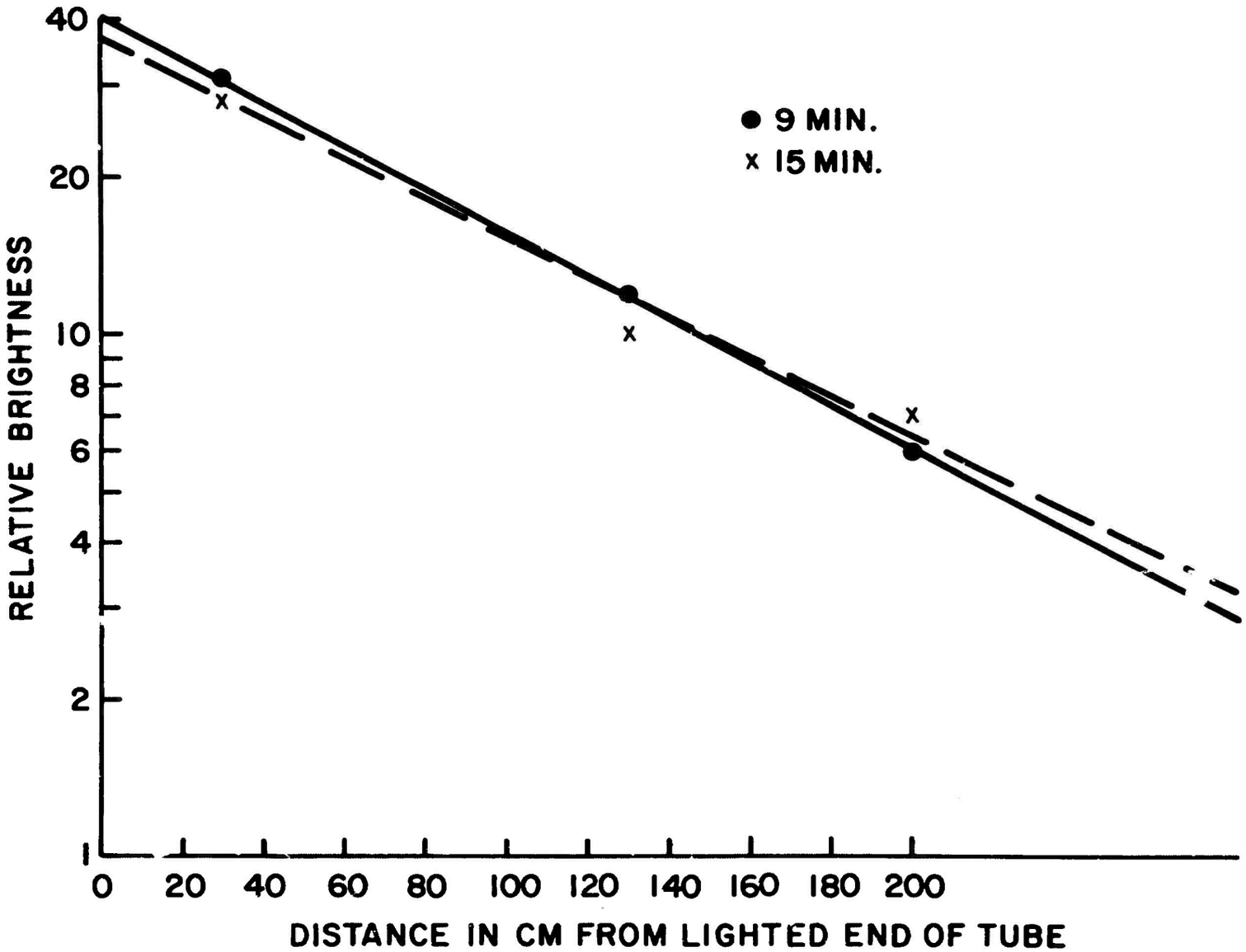

Fig. 13 The relative scattering intensity as a function of position along the tube axis nine minutes after dust injection, and 15 minutes after dust injection. The linearity (on a semilog plot) of the scattering for the nine minute data indicates that the dust concentration is uniform along the tube axis. The 15 minute data show that the scattering is beginning to show deviation, which indicates that the axial distribution is becoming less uniform.

a uniform dust mixture is being obtained along the horizontal tube.

3.2 Analytical Considerations

The energy scattered from a collimated beam of light by a cloud of dust particles is

$$E = \int_v \int_{\omega} \int_r I E_o n f \pi r^2 dr d\omega dv \qquad (1)$$

where I is the scattering coefficient, n is the local number of particles per unit volume, f is the size disbribution function, ω is the solid angle occupied by E, and v, and the volume of scattering particles.

The change in E_o can be obtained by the relationship

$$dE_o = E_o \epsilon n f \pi r^2 dr dx$$

where x is the depth into the scattering cloud and ϵ is the scattering efficiency. This gives

$$\ln \frac{E_o}{E'_o} = \int_x \int_r n f \pi r^2 \epsilon dr dx \qquad (2)$$

where E_o is the initial flux. The ratio $\frac{E_o}{E'_o}$ can be a function of radial position in the tube since the number of particles and f can be functions of axial as well as radial position.

Even though it is relatively simple to formulate equations 1 and 2 the relationship of data from measurements of energy to the actual number density requires much effort and involves additiona' uncertainty. The particle distribution function, f, must be known as well as ϵ and I (θ). To obtain ϵ and I (θ) the shape of the particles must be known. For pulverized material both f and the shape are not well known.

The distribution functions can be modeled and ϵ and $\iota(\theta)$ can be estimated either from theory or available data. This has been done by assuming that f is quadratic from r = o to a maximum at r_o and decreases exponentially thereafter. When this is above the scattering measurement and turbidity obtained from Figures 13 yield values of $.261 \times 10^{-2}$ particles / cm and $.336 \times 10^{-2}$ particles / cm respectively for $n r^2$. This coupled with the absolute value of the total mass of particles collected after evacuation yields a particle radius at which r_o is a maximum of about 2 microns which is in agreement with photomicrographs of the Teflon powder used.

3.3 Results and Discussion

For sufficiently small particles (our particle size is in the meighborhood of a micron) the gas which comes from the injector carries the small particles with it throughout the shock tube, so that if the dust is uniform in the injector it will be uniform anywhere in the shock tube. The data of Figure 13 indicate that the dust is evenly distributed. If the shock tube is fired within the first ten to fifteen seconds after the dust is injected, the uniformity in the vertical direction will be sufficiently constant to allow useful testing. This can be seen by observing the decay of light scattering from the regions near the top of the tube (Fig. 12). Of course, as soon as the dust enters a tube, there are portions of the shock tube which are beginning to be non-uniform in dust concentration starting from the top of the tube and working downwards. Within about fifteen seconds, for one centimeter initial shock tube pressure, the uniformity gradient in the vertical direction is zero except for a region about a few millimeters near the top of the tube. If the firing of the tube can be made automatic after the injection of the

powder, the uniformity will be even better than if the tube is fired manually because the firing of the tube can be accomplished more rapidly with an automatic system. Based upon the esults of the injection test, it appears entirely feasible to arrange the shock tube in a horizontal position and inject the dust from an intermediate, relatively high pressure volume.

BLANK PAGE

4. SHOCK TUBE MODIFICATION

From experience gained in the operation of the shock tube, and as a result of the data obtained in the powder injection test, several modifications have been made on the SAPAG device.

4.1 Injector Study Implications For Horizonal Operation

As mentioned in Section 3, the horizonal shock tube appears feasible if the tube can be fired immediately after dust injection. For this reason the shock tube has been mounted in a horizonal position. All sections of the tube are now steel, with quartz and glass windows available for instrumentation. The injector is located at one end of the tube in a similar fashion as used in the injector test. During operation the gas used for testing is placed in the injector. The shock tube itself is left evacuated and is isolated from the injector. Then the dust is injected into the injector housing and is finally placed in the shock tube by opening the inter-connecting valve. In this fashion all the gas that is to be used in the test is thoroughly mixed with the dust prior to placing it in the shock tube. This process accounts for the uniformity encountered in the injection process because dust imbedded in the gas tends to remain inbedded in that particular gas even when the pressure is drastically lowered.

The operational procedure in firing the shock tube has been arranged so that the tube can be fired immediately after the dust injection, with a minimum of elapsed time occurring between injection and firing.

4.2 Injector Vapor Barrier

The injector device described in Research Note 12 consisted of a large vacuum can in which a 12 inch speaker was

placed. The speaker is used to oscillate a sieve which contains the powder to be injected into the tube. With the new injection process the pressure in the injector housing is set slightly above the P_1 value desired in the shock tube and the injector is operated in the ordinary fashion. In addition, a fan has been placed underneath the sieve and is run during the in jection process. This simply stirs the injected dust thoroughly with the gas to be tested and after all of the dust is injected into the gas, the valve separating the injector housing and the shock tube is opened.

The speaker used in this process is a source of contaminants because the construction of the speaker requires the use of shellac and papers which tend to out-gas and produce water vapor, and relatively high vapor pressure organic materials. It was desired therefore to isolate the speaker from the powder being tested. This has been accomplished by placing a vacuum tight membrane across the end of the injector housing which allows only transverse motion. The system containing the speaker is still evacuated; however, the pressure achieved in this section is in the neighborhood of 40 or 50 microns. Figure 14 is a schematic drawing of the vapor barrier installed in the injector housing.

4.3 Vacuum System Improvements

The vacuum system has been modified to produce lower pressures in the test device. A new liquid nitrogen trap has been installed. With this addition the pumping system, including the trap and the inter-connecting plumbing, has a base pressure in the neighborhood of 1×10^{-6} millimeters of mercury. In the shock tube the base pressure is in the neighborhood of 5×10^{-6} millimeters of mercury. It is anticipated that during the next contract period

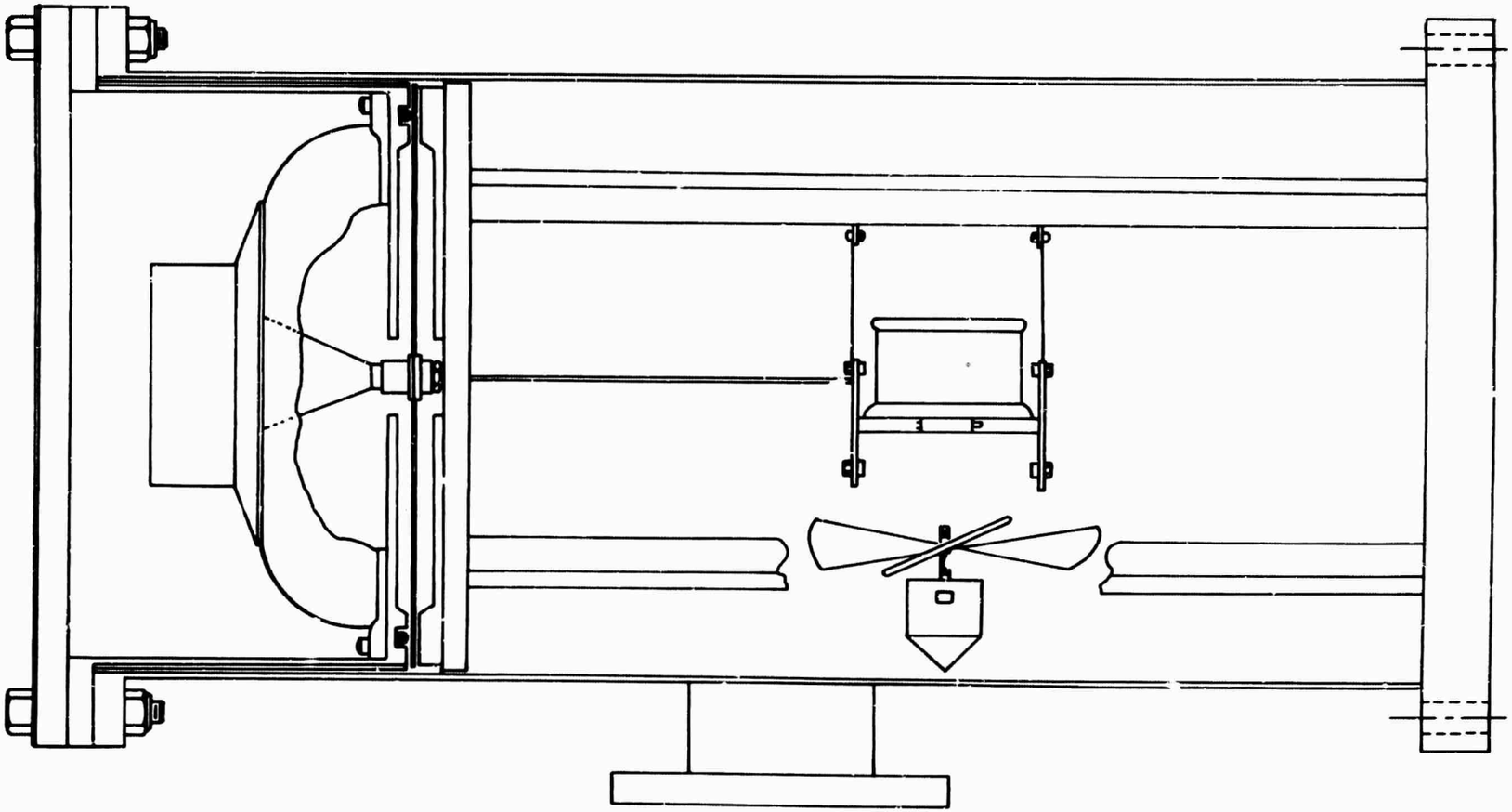

Fig. 14 Vapor barrier installed in the injector housing. A high vacuum is attained in the powder containing chamber while only a rough vacuum exists in the speaker chamber. Transverse motion is transmitted through a sealed stainless steel diaphragm.

flush vacuum valves will be obtained which allow large openings directly to high speed diffusion pumps. This will be especially important when production shots of ablation powders are being run because the ablation powders will produce high vapor pressure organic materials which will contaminate the system.

A mass spectrometric leak detector which has been added to the system has been very useful in improving vacuum operations.

5. INSTRUMENTATION

Considerable improvement has been made in instrumentation of the shock tube for measurement of ionization and radiation properties of ablation species. Data can be obtained on a better quantitative basis and more comprehensive coverage of observables is possible for each run.

5.1 Electron Density

A new induction coil has been completed for the measurement of electron number density. The electronic parameters of the new coil are the same as those of the previous coil; however, the new device is encased in a metal tube and can be used over a much higher range of shock strengths.

5.2 Radiation

The various photomultiplier tubes and the indium-antimonide infrared detector in use are fitted with interference filters which define band-passes so that quantitative intensities are obtained, and which permit observations within band systems of interest. The phototube-filter combinations have been calibrated against a standard lamp so that measurements can be reduced to an absolute basis.

A half-meter Ebert mounting spectrograph has been fitted with a rotating sector which scans the slit during a period that corresponds to shock radiation duration and gives time resolved emission spectra. An E. G. and G. flash lamp has been added for use with this instrument so that time resolved absorption spectra can be obtained similarly.

A Jarrell-Ash f/6.3 spectrograph has been added to the instrumentation, including a photoelectric attachment for obtaining

finely time resolved intensity measurements. In addition, an arc and spark unit has been mounted for obtaining reference spectra. A small tungsten filament lamp, calibrated against our N. B. S. tungsten filament standard lamp, has also been set up as a working standard.

Data recording has been facilitated by the aquisition of additional Tektronix type 535 and 555 oscilloscopes with Polaroid cameras.